Effective Charge of Adsorbed Poly(amidoamine) Dendrimers from Direct Force Measurements

Ramon Pericet-Camara,[†] Georg Papastavrou,* and Michal Borkovec

Department of Inorganic, Analytical, and Applied Chemistry, University of Geneva, Sciences II, 30, Quai Ernest-Ansermet, 1211 Geneva 4, Switzerland

Received October 22, 2008; Revised Manuscript Received December 20, 2008

ABSTRACT: Interaction forces between silica surfaces with adsorbed poly(amidoamine) (PAMAM) dendrimers were measured with the colloidal probe technique based on the atomic force microscope (AFM). At small separations, attractive non-DLVO forces are observed. These forces likely originate from interactions between oppositely charged patches on the surfaces, resulting from the heterogeneous distribution of the adsorbed positively charged dendrimers on the negatively charged surface. At large separation distances, the interaction forces are repulsive and consistent with DLVO theory. These forces can be interpreted quantitatively as originating from the overlap of diffuse layers of positively charged surfaces in terms of the Poisson−Boltzmann theory. From the resulting diffuse layer potentials, one can extract the effective charge of the dendrimers in the adsorbed state. This effective charge is about half of the ion condensation value given by Poisson−Boltzmann theory for a charged spherical macromolecule in solution for the different dendrimer generations investigated. This reduction probably originates from the smaller volume available for the diffuse layer of adsorbed macromolecules, but charge neutralization may also play an essential role.

Introduction

Polyelectrolytes are widely used as additives in industrial applications, for example, in food processing, cosmetics, papermaking, or wastewater treatment.[1−6] The principal role of these additives is to tune the interaction forces between the particle surfaces and thereby to control the stability of the particle suspensions in question.[7,8] Cationic polyelectrolytes are frequently used to destabilize colloidal particle suspensions due to their strong adsorption affinity to negatively charged surfaces. When such polyelectrolytes are properly dosed, one can neutralize the surface charge and thereby induce attractive forces between particles, which lead to particle aggregation and to destabilization of the colloidal suspension. At higher polymer doses, stable suspensions can be obtained. Under such conditions, the adsorption process reaches saturation and the surface charge reverses its sign.[9,10] Such overcharged surfaces repel strongly due to overlapping electrical double layers.

The interaction forces in such systems appear to be in line with the theory of Derjaguin, Landau, Verwey, and Overbeek (DLVO).[11−14] This classical theory decomposes interactions between identical colloidal particles in an electrolyte solution into attractive van der Waals forces and repulsive electrostatic double layer forces. At the charge neutralization point, the double layer forces vanish and the van der Waals forces lead to a net attraction. Away from the charge neutralization point, the double layer forces dominate, and lead to overall repulsion.

This scenario has been qualitatively confirmed with colloidal dispersions in the presence of oppositely charged polyelectrolytes, mainly through electrophoresis and light scattering.[7,8,15−20] However, several of these studies indicate that one cannot easily rationalize the magnitude of the DLVO forces, whose strength is related to the diffuse layer charge of the overcharged surface.[15,18,19] Moreover, the presence of additional attractive non-DLVO forces has been pointed out. Some authors suggested that these attractive interactions originate due the heterogeneous patch−charge distribution, which is expected when highly charged polyelectrolytes adsorb to a weakly charged surfaces.[7,8,18] Others have argued in favor of attractive forces originating from bridging of individual polymer strands between the surfaces.[19,20]

In order to address the validity of DLVO theory and to clarify the origin of eventual non-DLVO forces, several authors focused on direct force measurements between surfaces in the presence of oppositely charged polyelectrolytes.[21−25] These studies have clearly confirmed that at high polyelectrolyte dose surfaces repel due electric double-layer forces, which are in accord with DLVO theory. These forces are often strongly repulsive, but currently no accepted approach seems to exist to estimate their magnitude from the adsorbed amount and the properties of the polyelectrolyte. Moreover, these forces often remained repulsive down to contact, showing no sign of any attractive forces. Attractive forces were reported based on direct force measurements close to the charge neutralization point involving macroscopic surfaces, but typically only in the initial stages of the experiments.[21−24] Nevertheless, these studies have revealed that attractive forces in polyelectrolyte systems cannot be always described with classical DLVO theory, and that they are often stronger than van der Waals forces. On the basis of direct force measurements, these non-DLVO forces were usually attributed to polymer bridging.

While direct force measurements are simpler to interpret than colloidal stability data, pinpointing the mechanism of interaction forces acting between surfaces with adsorbed linear polyelectrolytes remains difficult. Such adsorbed films contain large amounts of counterions of the polyelectrolyte,[15,25,26] and their diffuse layer charge cannot be simply estimated from charge balance arguments. With the atomic force microscope (AFM) it became not only possible to image the laterally heterogeneous and patchy structure of these films,[27] but also to demonstrate the existence of individual bridging polymer chains.[25,28−30] However, how to transform these interesting results into a predictive tool of interaction forces between macroscopic surfaces or between colloidal particles remains far from obvious.

Interaction forces in the presence of branched polyelectrolytes should provide additional evidence concerning the role of

* Corresponding author: Telephone: +41 22 379 6429. Fax: +41 22 379 6069. E-mail: georg.papastavrou@unige.ch.

[†] Present address: Department of Applied Physics, University of Granada, Avenue Severo Ochoa, 18071 Granada, Spain.

10.1021/ma802374z CCC: $40.75
Published on Web 02/13/2009

polymer bridging forces and the charge balance in adsorbed polyelectrolyte films. The contribution of an individual branched polyelectrolyte to the charge balance of the adsorbed film is easier to rationalize than for linear chains. Furthermore, bridging forces should be much less important. While such studies are rare, branched poly(ethyleneimine) (PEI) was studied in some detail.[8,21,31] Negatively charged colloidal particles undergo a charge reversal in the presence of PEI, and the system behaves similarly to linear polyelectrolytes.[8] From direct force measurements in the presence of PEI one knows that strongly repulsive double layer forces occur at high polymer dose, while attractive non-DLVO forces were observed near the charge reversal point.[21,31] However, the adsorbed PEI films are unusually homogeneous close to saturation conditions. This homogeneity is possibly related to the polydispersity of the samples, and this makes identification of individual PEI molecules on the surface difficult.[32,33] For these reasons, obtaining more detailed information on the interaction mechanism in this system has not been achieved so far.

Another interesting class of branched polyelectrolytes are charged dendrimers, which are tree-like globular macromolecules with a dense core.[34,35] In the present context, cationic poly(amido amine) (PAMAM) dendrimers are most interesting, as they are available with low polydispersity and over a wide range of generations.[34−36] In mildly acidic conditions, PAMAM dendrimers are highly positively charged.[37] Many studies have demonstrated that cationic dendrimers adsorb strongly to oppositely charged substrates.[38−42] Higher generations of PAMAM dendrimers can be easily imaged by AFM on many substrates, and therefore information on the adsorbed amount and their lateral arrangement can be obtained. Such studies indicate that adsorbed dendrimers form liquid-like monolayers with relatively low surface coverage even for extended adsorption times. Many features of the adsorption process can be explained in terms of random sequential adsorption (RSA).[43−45] Electrophoresis and light scattering studies further demonstrate that charged particle dispersions in the presence of oppositely charged dendrimers behave similarly as in the presence of linear or other branched polyelectrolytes.[42,46] With increasing dendrimer dose, the particles undergo a charge reversal and the existence of additional attractive non-DLVO forces has been proposed. The position of the charge reversal point for PAMAM dendrimers adsorbed on latex particles could be approximately rationalized by considering the counterion condensation within Poisson−Boltzmann (PB) theory.[46]

The present article explores the idea to use dendrimers to model the adsorption of branched polyelectrolytes further. In particular, we study interaction forces between silica surfaces in the presence of PAMAM dendrimers with the colloidal probe technique. Interaction forces between surfaces coated with adsorbed dendrimers have not yet been studied in much detail.[47,48] These studies have confirmed the existence of attractive force at low dendrimer dose, and reported strong repulsion consistent with a double layer force at higher dose. However, these studies focused on low generation dendrimers, and the force measurements could not be related to the structure of the adsorbed dendrimer layers. In the present study, however, we make a detailed link between the measured forces and layer structure. In particular, the effective charge of the dendrimers in the adsorbed state will be measured. For the first time, we show how the magnitude of repulsive forces acting between adsorbed polyelectrolyte layers can be estimated from the charge of the polyelectrolyte and its geometrical dimensions.

Materials and Methods

Dendrimer Adsorption. PAMAM dendrimers of generations G6, G8, and G10 were obtained as aqueous solutions from Dendritech (Midland, MI). The concentration of the dendrimer solution was verified by total carbon and nitrogen analysis (Shimadzu TOC-V). Fresh dendrimer solutions were prepared in the concentration range of 5−10 mg/L and they were adjusted to pH 4 by addition of HCl and to the desired ionic strength by addition of KCl. Millipore water was used throughout.

Dendrimers were adsorbed to planar silica substrates and to colloidal probes. The silica substrates were planar silicon wafers with a natural oxide layer (SiO_2) obtained from Silchem (Freiberg, Germany). The oxide layer has a thickness of about 5 nm as verified by null ellipsometry in air. The silicon wafers were cleaned by the RCA method before use.[49] This procedure consists of heating a 1:1:5 mixture of hydrogen peroxide (30%), ammonia (24%), and water with the wafer at a temperature of 80 °C for 10 min. Subsequently, the wafers were rinsed and stored until further use in water for less than 24 h.

Colloidal probes were prepared by mounting colloidal silica particles with an average diameter of 6−7 μm (Bangs Laboratories) on tip-less AFM cantilevers (CSC 12, MikroMasch, Estonia). The particles were attached with UV-curable glue (NO 68, Norland adhesives) under an optical microscope by means of a micromanipulator. The glue was cured directly under the microscope by means of a mercury lamp.

Adsorption of dendrimers was realized for flat substrates and for colloidal probes as follows. Prior to adsorption, the wafers and the colloidal probes were cleaned in air plasma at 35 W for 5 min (Harrick Scientific, NY). Both substrates were immersed in the dendrimer solution of pH 4 and of adjusted ionic strength for about 12 h. This time is sufficient to reach the adsorption plateau at the respective dendrimer concentration.[43] After adsorption, the wafers and the colloidal probes were transferred for approximately 1 min to Millipore water and subsequently dried in a stream of nitrogen. The procedure resulted in a homogeneous distribution of the dendrimers over the sample area on either substrate.[43,50]

AFM Imaging. Adsorbed dendrimers were imaged in air in tapping mode with a Multimode Nanoscope III AFM (Veeco, Santa Barbara, CA) using an J-scanner and standard tapping cantilevers (OMCL-AC160TS-W2, Olympus, Japan). For flat substrates, at least five different positions on the sample were analyzed. For each adsorption condition, 500−1500 dendrimers were imaged by scanning an area of 1 × 1 μm. Their number density and lateral positions were obtained with an image analysis package developed in-house, which is based on previously published algorithms.[43,51] The fractional surface coverage was calculated from the number density of the adsorbed dendrimers and their geometrical dimensions.[43] The pair correlation functions were calculated by binning the radial distances between the positions of at least 500 denrimers in the AFM images.

For these experiments, silica particles were attached to silicon wafers in an analogous manner as to the tip-less cantilevers. The roughness of the bare substrates was determined from the root-mean-square (rms) deviation of the surface profile. To obtain the rms roughness of the colloidal particles, the spherical profile of the particle was subtracted from the image first.

Direct Force Measurements. Direct force measurements were performed with a MFP-3D (Asylum Research, Santa Barbara, CA). The wafer and the colloidal probe to which dendrimers were adsorbed under identical conditions were mounted in a Petri dish filled with electrolyte solution of appropriate ionic strength and pH 4. Before the force measurements, the system was allowed to equilibrate for about one hour at room temperature. Under these conditions, the adsorbed dendrimer film remains stable over periods of at least several hours. The stability of the adsorbed films was explicitly verified for the planar silica substrates by reflectometry,[45] and we assume that the colloidal silica probes behave analogously. Direct force measurements were performed with approach and retraction velocities in the range of 0.2−0.6 μm/s. During one measurement cycle, at least 50 curves were accumulated for one position, and such a cycle was repeated for at least three different positions. No significant variation in the long-ranged forces was observed between the different positions, confirming the lateral

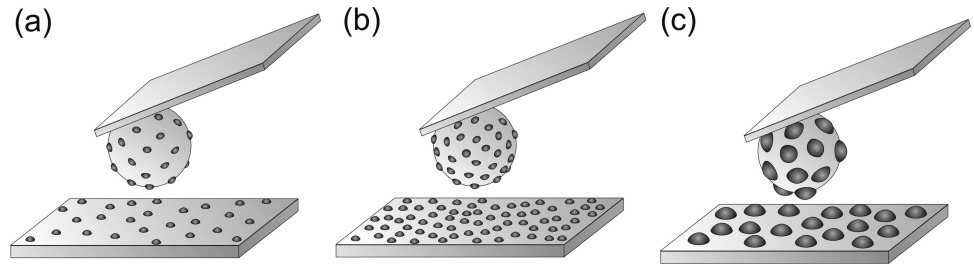

Figure 1. Schematic representation of the direct force measurements between negatively charged silica surfaces coated with positively charged dendrimers. By variation of the adsorption conditions one can obtain (a) low and (b) high surface coverage, while with dendrimers of different generations one can obtain charged patches of (b) smaller and (c) larger size and charge.

homogeneity of the samples. For each condition, the force curves were averaged to improve the signal-to-noise ratio. For a given surface coverage and dendrimer generation, force measurements were performed for at least three different ionic strengths.

The deflection versus piezo-displacement curves were converted to force versus distance curves by standard procedures.[52] The separation distance was determined with respect to the onset of the constant compliance region. In this region, the force response of the cantilever is linear with the piezo displacement, and can be clearly identified for thin polymer layers.[24,31] The force constant of the cantilever was determined from the deflection amplitude due to the thermal noise.[53] The resulting values were compared to the ones obtained by a method based on hydrodynamic properties of the cantilever.[54] The force constants were in the range of 0.02−0.1 N/m and they did not deviate more than 25% for the different methods. The force F was converted to normalized forces F/R by dividing with the radius R of the colloidal probe. The radius of the probe was determined by means of optical microscopy with an accuracy of about 0.3 μm. The normalized force profiles were fitted at large separation distances to the full solution of the PB equation for different boundary conditions.[13,55] In order to avoid the influence of patch charge attraction and charge regulation on the diffuse layer potentials, the fits were restricted to separation distances exceeding two times the expected Debye length.

Results and Discussion

Well-defined heterogeneously charged surfaces were obtained by adsorption of positively charged PAMAM dendrimers to negatively charged silica. Interaction forces between such surfaces were measured with the colloidal probe technique (Figure 1). Since the system is symmetric to good approximation, one can extract the diffuse layer potential of the surface by fitting the force profile to the solution of the PB equation. The effective charge of an adsorbed dendrimer is obtained from the measured potentials with a simple smeared-out charge model.

Properties of Adsorbed Dendrimer Layers. Parts a and b of Figure 2 show the surface topography of the silica substrates after adsorption of PAMAM dendrimers at pH 4 and ionic strengths of 0.1 mM and 5.0 mM, respectively. The surface topography has been obtained by AFM imaging in tapping mode for dried samples. The phase response given in gray scale is superposed to the spatial representation of the surface topography. The phase signal is sensitive to the viscoelastic and adhesive properties of the sample and leads to better contrast between the soft dendrimers (dark regions) and the hard silica surface (bright regions). These images confirm that the dendrimers flatten substantially upon adsorption and that their radius in the adsorbed state increases with respect to their radius in solution (see Table 1).[43,56]

Adsorption of dendrimers to colloidal silica particles reveals similar trends. The corresponding images are shown in Figure 2, parts c and d. Dendrimers adsorbed to these silica particles cannot be localized through their topography due to the roughness of the particles, but they can be clearly identified by the phase signal. Bright areas in the phase signal indicate the hard silica surface, while the gray areas indicate the dendrimers. The black areas in the phase signal of Figure 2c result from the large phase shift in deep valleys on the rough particles, as the phase signal is partly convoluted with the surface topography. The roughness of the silica particles with a root-mean-square (rms) deviation of about 1.8 nm is indeed larger than for the planar silica substrate with an rms value of about 0.2 nm.[50,57] Differences in the apparent dimensions of the dendrimers between these two images are due to the different tip curvature radii of the AFM cantilevers used. While the dendrimers have the same size, a tip with a larger curvature radius will lead to larger apparent dimensions due to tip convolution effects.

By comparing these images, one further observes that the surface coverage of dendrimers increases with increasing ionic strength. To discuss this dependence in more detail, let us represent the surface coverage as a function of the screening parameter κa, where a is the dendrimer radius in the adsorbed state and κ is the inverse Debye length given by[13]

$$\kappa = \sqrt{\frac{2N_A e^2 I}{\epsilon\epsilon_0 kT}} \tag{1}$$

where N_A is Avogadro's number, e is the elementary charge, I is the ionic strength in mol/L, $\varepsilon\varepsilon_0$ is dielectric permittivity of water and kT is the thermal energy at room temperature. The radii a of dendrimers in the adsorbed state have been determined by AFM, and the values for different generations are summarized in Table 1.[43] Since the number density n of adsorbed dendrimers can be accurately estimated by counting the dendrimers on the AFM images, the surface coverage can be evaluated as

$$\theta = \pi a^2 n \tag{2}$$

While the relationship is only applicable to monodisperse samples, the effects introduced by the minor polydispersity of the dendrimers can be neglected to a good approximation.[39,43]

Figure 3 shows that the surface coverage θ increases with increasing screening parameter κa for different silica substrates and for different dendrimer generations. This increase reflects an increase of the surface coverage with the ionic strength, since the screening parameter is proportional to the square root of the ionic strength. For flat substrates, G8 and G10 dendrimers fall on the same master curve. Adsorption of the G10 dendrimers on the colloidal particles leads to very similar coverage as for the flat substrates, which confirms that these two silica substrates behave very similarly. The measured surface coverage is close to the one determined by reflectometry under similar conditions.[45]

In order to estimate the fractional surface coverage for different adsorption conditions and generations, we interpolate the experimental data in a heuristic manner by an exponential

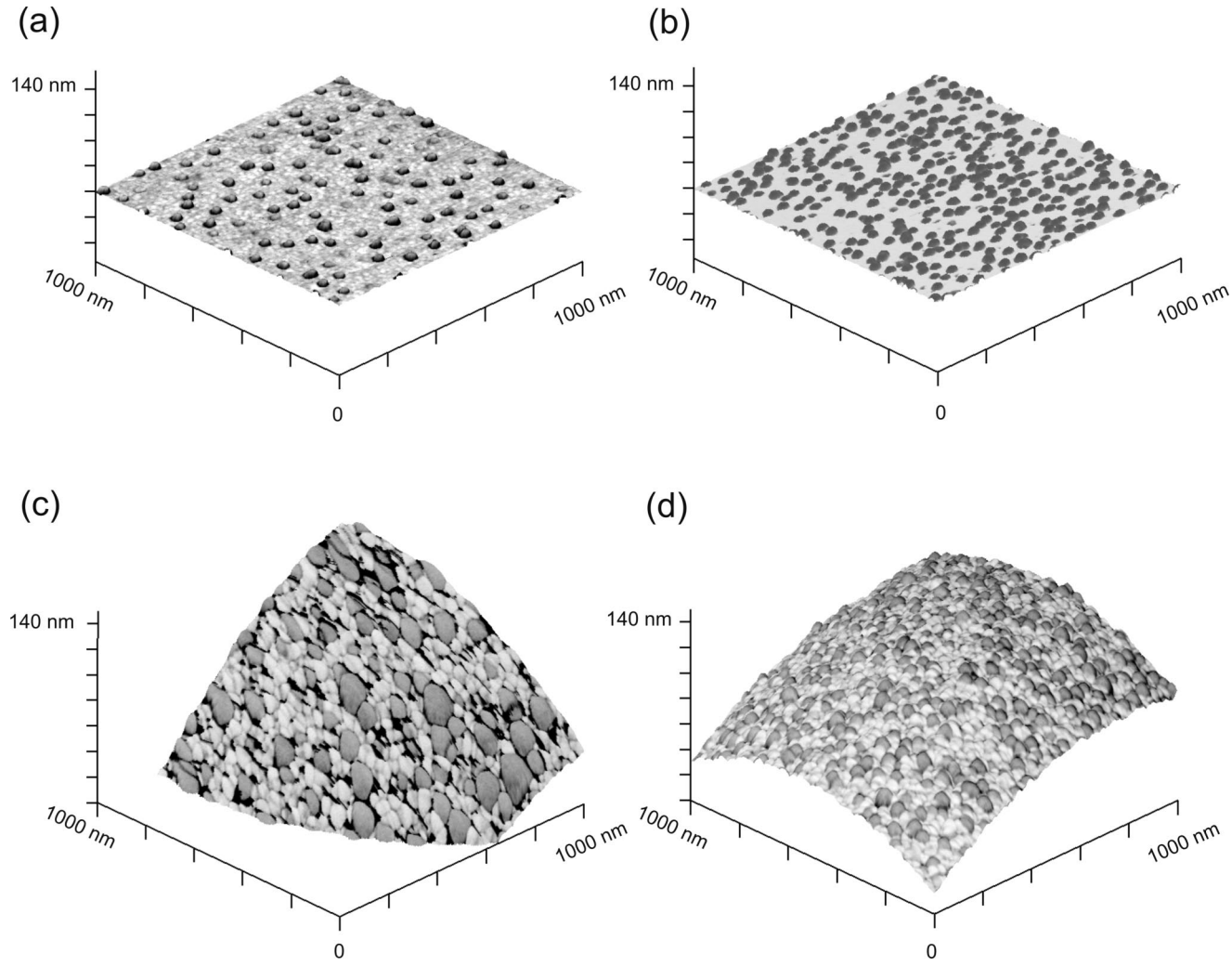

Figure 2. AFM images of PAMAM G10 dendrimers adsorbed to (a, b) flat silica substrates and (c, d) colloidal silica particles. The topography of the sample is represented spatially, while the gray scale represents the phase shift. The dark areas correspond to dendrimers. Adsorption has been performed at pH 4 and ionic strength of (a, c) 0.1 mM and (b, d) 5 mM.

Table 1. Geometrical Dimensions of PAMAM Dendrimers

	molecular mass (kDa)[a]	radius in solution (nm)[a]	radius in adsorbed state (nm)[b]
G6	58	3.35	3.35[c]
G8	233	4.85	6.35
G10	935	6.74	9.15

[a] As reported by the manufacturer. [b] Values obtained from AFM-images of adsorbed dendrimers of generations G10 and G8.[43] [c] The radius in the adsorbed state appears to be similar to the radius in solution.

function. This empirical fit function resembles the prediction of the random sequential adsorption (RSA) model based on three-body electrostatic interaction,[45] but provides a more accurate interpolation of the experimental data that is needed here. The random sequential adsorption model (RSA) assumes that the dendrimers adsorb irreversibly in a sequential manner at random positions without overlap. In the case of charged dendrimers the radius entering the classical RSA model has to be replaced by an effective radius to account for the electrostatic repulsion between the charged dendrimers. It has been recently demonstrated that the influence of the substrate has to be taken into account.[45] It is important to notice that the RSA-adsorption is a nonequilibrium process and that no redistribution or desorption of the dendrimers is taking place. The heuristic curve shown in Figure 3 will be used to estimate the surface coverage for the different dendrimer generations, including G6, which cannot be imaged easily on the silica substrates used. Therefore,

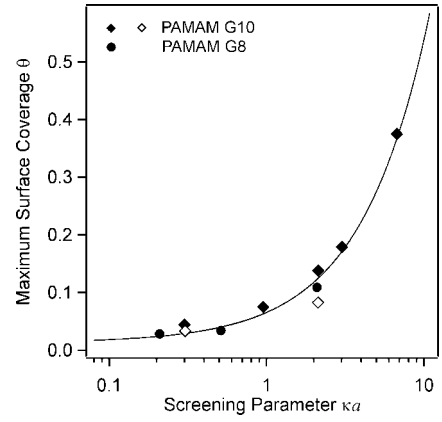

Figure 3. Maximum surface coverage θ of adsorbed PAMAM dendrimers on silica substrates at pH 4 as function of the screening parameter κa. Thereby, θ is the inverse Debye length and a is the radius of the dendrimers in the adsorbed state. The experimental data are compared for flat substrates (solid symbols) and colloidal particles (open symbols). The solid line represents an empirical fitting function.

we assume that for G6 the radii in the adsorbed state and solution are approximately the same.

Dendrimers adsorb on solid substrates in monolayers of liquid-like structure. This structure is revealed by the peak in the pair distribution functions of the adsorbed G10 dendrimers

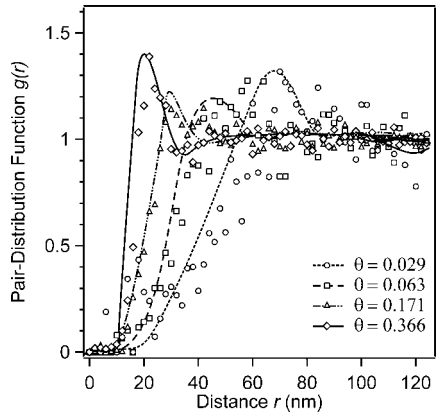

Figure 4. Radial pair distribution function $g(r)$ for adsorbed PAMAM G10 dendrimers adsorbed to a silica surface at pH 4 for different surface coverage. The lines serve to guide the eye only.

on flat silica substrates in Figure 4. The position of the maximum in the distribution function reflects the distance between nearest neighbors, and this distances decreases with increasing ionic strength. This decrease originates from the corresponding decrease of the Debye length, which determines the range of the screened Coulomb repulsion between the dendrimers. The same effect is responsible for the increase of the surface coverage with increasing ionic strength. Such electrostatic effects are well documented for irreversible adsorption on solid substrates within the RSA model for dendrimers[43,45] and for colloidal particles.[58−61] This adsorption mechanism further explains why the roughness of the substrate is unimportant. The overall surface coverage is determined by electrostatic repulsion between the dendrimers, and the substrate roughness only influences the details of the final adsorption spot. We suspect that the long-range nature of the interaction potential is the main reason why the structure of the adsorbed dendrimer layers is similar for the planar silicon wafer and for the colloidal silica particles in spite of their differences in roughness.

Adsorption of dendrimers of generation G6 through G10 to oppositely charged surfaces is irreversible at pH 4 and the low ionic strengths considered. This point was demonstrated by reflectivity studies where it was shown that rinsing the substrate with a dendrimer-free solution leads to no desorption of the adsorbed dendrimers.[45] The liquid-like arrangements of the dendrimers on the surface observed by AFM provide another piece of evidence. If the dendrimers were mobile, they are expected to crystallize in a two-dimensional lattice.[62]

Interaction Forces between Dendrimer-Coated Surfaces. The colloidal probe technique was used to measure interaction forces between surfaces with preadsorbed PAMAM dendrimer layers. The measurements were carried out in pure electrolyte solutions at pH 4 and various ionic strengths adjusted with KCl. In the employed sphere-plane geometry, the adsorbed layers were prepared prior to the measurement by adsorption from solution to the flat substrate and to the colloidal probe. As discussed above, such preadsorbed layers are irreversibly adsorbed and remain stable in dendrimer-free electrolyte solutions over several hours for all conditions used. This point was explicitly verified by reflectometry for the planar substrates,[45] and we surmise that adsorbed dendrimers layers are ever more stable on colloidal particles due to their larger roughness. The force measurements were carried out for different dendrimer generations and for different surface coverages θ. The coverage was varied by adjusting the ionic strength during adsorption. Note that the ionic strength, at which the forces were measured, was not necessarily the same as the ionic strength used during adsorption.

Figure 5 shows few representative approach and retraction force profiles for surfaces coated with G10 dendrimers measured in dendrimer-free electrolyte solutions of pH 4 without added salt for different fractional surface coverage θ. The resulting ionic strength of the solution is near 0.1 mM. The data include the bare silica surfaces with $\theta = 0$ (Figure 5a) and surfaces coated with dendrimers with a coverage of $\theta = 0.048$ and $\theta = 0.145$ (Figure 5, parts b and c).

For the bare silica surfaces, the interaction forces are weakly repulsive over the whole separation range upon approach and retraction (Figure 5a).[63] Attractive van der Waals forces are expected to lead to a jump-in instability at distances of 1−2 nm upon approach, and to an adhesion peak upon retraction. The absence of these instabilities is well-known for silica surfaces,[50,64] and probably originates from surface roughness or the presence of a gel-like layer of polysilicic acid chains protruding from silica surfaces into the solution.

For surfaces coated with dendrimers, repulsive forces due to diffuse layer overlap are much stronger than for the bare surfaces, indicating a higher surface charge of the dendrimer-coated surfaces. Moreover, the strength of the repulsion increases with increasing coverage. In contrast to the bare silica surfaces, characteristic jump-in instabilities are evidenced upon approach. At the same time, pronounced adhesion peak is observed upon retraction. The latter observations point toward additional attractive forces acting between the adsorbed dendrimer layers.

Forces upon Approach. The force profiles measured upon approach were analyzed for different ionic strengths, dendrimer coverage, and dendrimer generations. Figures 6 and 7 show typical force profiles normalized to the particle radius for surfaces coated with PAMAM dendrimers at different ionic strengths. The exponential nature of these forces at larger distances and the decrease of their range with increasing ionic strength indicate that these repulsive forces result from the overlap of diffuse layers. Such forces are expected from DLVO theory for charged surfaces, and they will be discussed in detail below. Each force profile originates from the averaging of 30−50 single force curves, which are acquired at the same lateral position. The parts of the force curves dominated by the repulsion between the diffuse layers do not vary significantly from curve to curves. Moreover, the force profiles were measured for at least three different positions on the sample and at larger distances the variation of the forces remained within 20%.

At shorter distances, one observes a jump-in for separations typically in the range of 5−15 nm. The distances and occurrence of such jump-ins are quite erratic, and they depend on the relative position of the probe and of the substrate. We suspect that these instabilities originate from the attraction between heterogeneously patch-charged surfaces. These non-DLVO forces have been suggested to be exponential with a range of half of the Debye length or possibly smaller.[5,65,66] The latter situation may occur if the Debye length exceeds the characteristic size of the surface heterogeneities. The large variations are probably caused by the substantial variation of these forces with the relative lateral position of the surfaces.[65]

Figures 6 and 7 further demonstrate that the measured forces are in agreement with DLVO theory. The solid lines are fits with numerical solutions of the PB equation for constant charge (CC) boundary conditions. Figures 6a compares these results with the constant potential (CP) boundary conditions. As the solution is obtained for two plates, comparison with the experimental data invokes the Derjaguin approximation.[13,14] While this approximation might be questioned for heterogeneously charged surfaces, its validity has been confirmed experimentally in a very similar system.[50] The present fits were restricted to separation distances larger than two times the

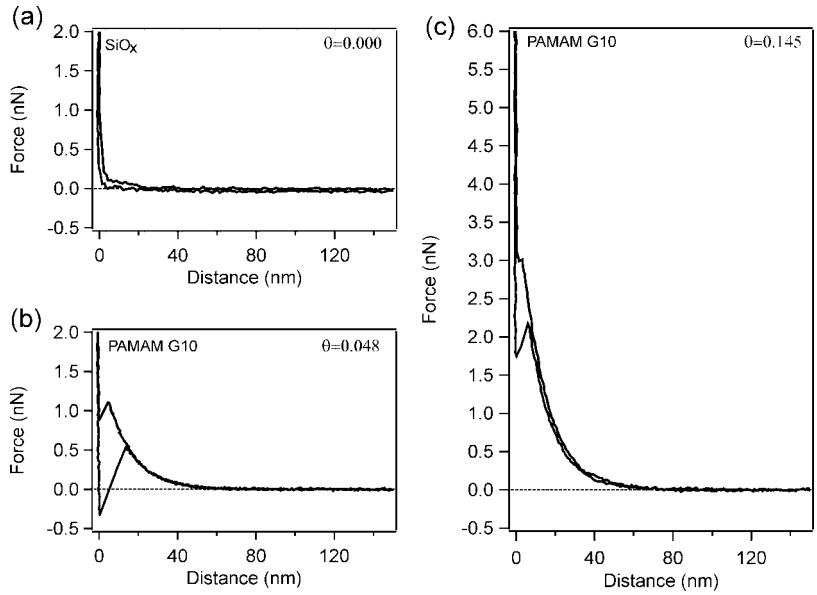

Figure 5. Representative force profiles measured between silica surfaces with adsorbed dendrimers PAMAM G10 at pH 4 and an ionic strength of 0.6 mM. The different graphs represent the forces for (a) bare surfaces ($\theta = 0$), and two different surface coverages (b) $\theta = 0.048$ and (c) $\theta = 0.145$.

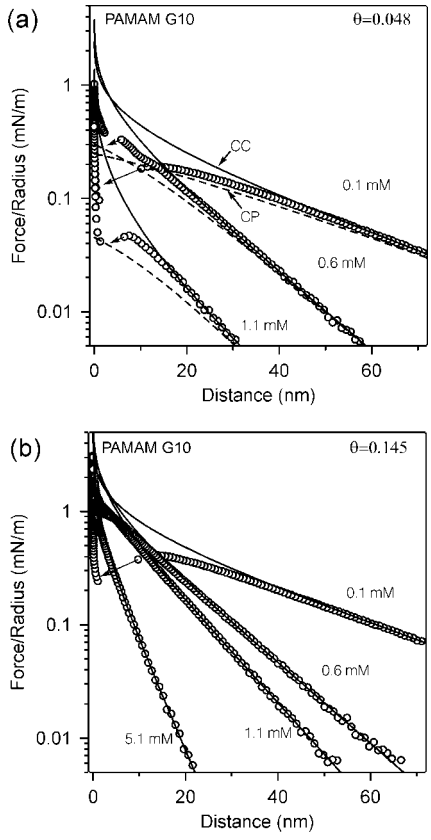

Figure 6. Force profiles upon approach for silica surfaces coated with adsorbed PAMAM G10 dendrimers at pH 4 and different ionic strengths. The data are shown for (b) low $\theta = 0.048$ and (c) high $\theta = 0.145$ surface coverage. Arrows indicate jump-ins due to attractive forces. The solid lines are results of calculations with PB theory with constant charge (CC) boundary conditions. The broken lines in part a are based on constant potential (CP) boundary conditions.

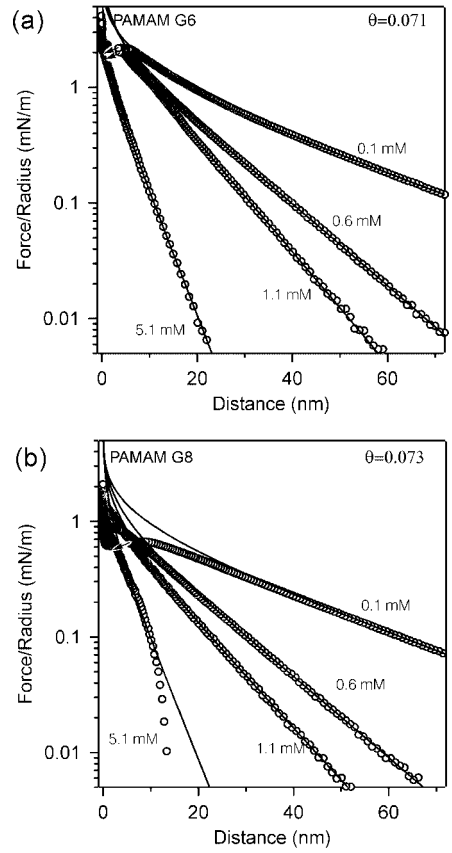

Figure 7. Force profiles upon approach for silica surfaces coated with adsorbed PAMAM G10 dendrimers at pH 4 and surface coverage of $\theta \approx 0.07$ at different ionic strength. The data are shown for generations (a) G6 and (c) G8. Arrows indicate jump-ins due to attractive forces. The solid lines are results of calculations with PB theory with constant charge (CC) boundary conditions.

expected Debye length. At these distances, the diffuse layer potentials are basically independent from the boundary conditions chosen. Due to the presence of additional attractive forces, no attempt is made to obtain further information on the appropriate boundary conditions, and any eventual effects of charge regulation.[13,55] Due to the thickness of adsorbed dendrimers of a few nanometers, the planes of origin of the positive charge localized on the dendrimers and of the charge of the silica substrate are not identical, and this difference may equally lead to deviations from the solutions of the PB equation,

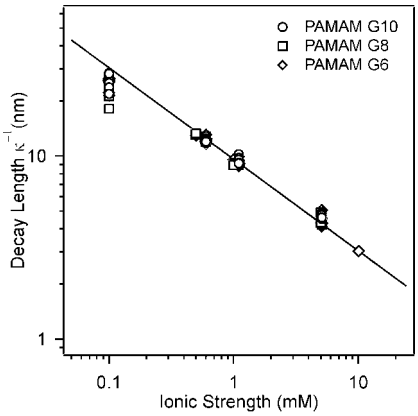

Figure 8. Decay length of the repulsive forces as a function of the ionic strengths for silica surfaces coated with PAMAM dendrimers of different generations at pH 4. The solid line is the theoretical Debye length (see eq. 1).

especially at small distances and higher ionic strengths. One should equally note that van der Waals forces are negligible at the distances considered.

Figure 6 shows the influence of the surface coverage for PAMAM G10 dendrimers. One observes that the force becomes more repulsive with increasing coverage, indicating that the diffuse layer potential increases with increasing dendrimer loading. At an ionic strength of 0.1 mM, the diffuse layer potential increases from +40 mV at $\theta = 0.048$ to +79 mV at $\theta = 0.145$. This increase can be explained by the fact that the dendrimers are positively charged, and an increase in the adsorbed amount will lead to higher surface charge and higher surface potential.

While this interpretation assumes that the overall surface potential is positive, its sign cannot be inferred in symmetric systems from such force measurements. Nevertheless, the positive sign of the surface potential is confirmed by the increase of the magnitude of the diffuse layer with increasing coverage. If the reverse were true, its magnitude would decrease. The fact that the surface is positively charged is not surprising. The surface charge of silica is negative, but at pH 4 its magnitude is relatively small.[63,67,68] On the other hand, the dendrimers are fully protonated and thus highly positively charged.[37] Due to the strong affinity of charged dendrimers to oppositely charged surfaces, one expects a charge reversal for a sufficiently high coverage. This charge reversal or overcharging has been documented for PAMAM dendrimers for sulfate latex particles.[46] Similar charge reversal phenomena have been described for various polyelectrolytes adsorbed on oppositely charged surfaces.[5,7,15,19]

Figure 7 shows the variation of the forces with the dendrimer generation, and one observes that the strength of the interaction decreases with the dendrimer generation at constant coverage. At an ionic strength of 0.1 mM, the diffuse layer potential decreases from +97 mV for G6 to +66 mV for G8. This trend originates from the progressive neutralization of the dendrimer charge with anions bound in the interior of the dendrimer.

Figure 8 shows the decay length obtained from fits to the PB equation as a function of the ionic strength. The solid line represents the expected Debye length (see eq. 1). In general, one finds a good agreement between the experimental values and the theoretical curves for all surface coverage and dendrimer generations. Only at the lowest ionic strengths, the measured decay lengths are smaller than expected. These discrepancies indicate that the ionic strength of the solution is actually somewhat higher than for water adjusted to pH 4. At this low ionic strength, one may expect that the solution accumulates additional ions originating from dissolution of carbon dioxide or leaching out of glass vessels.

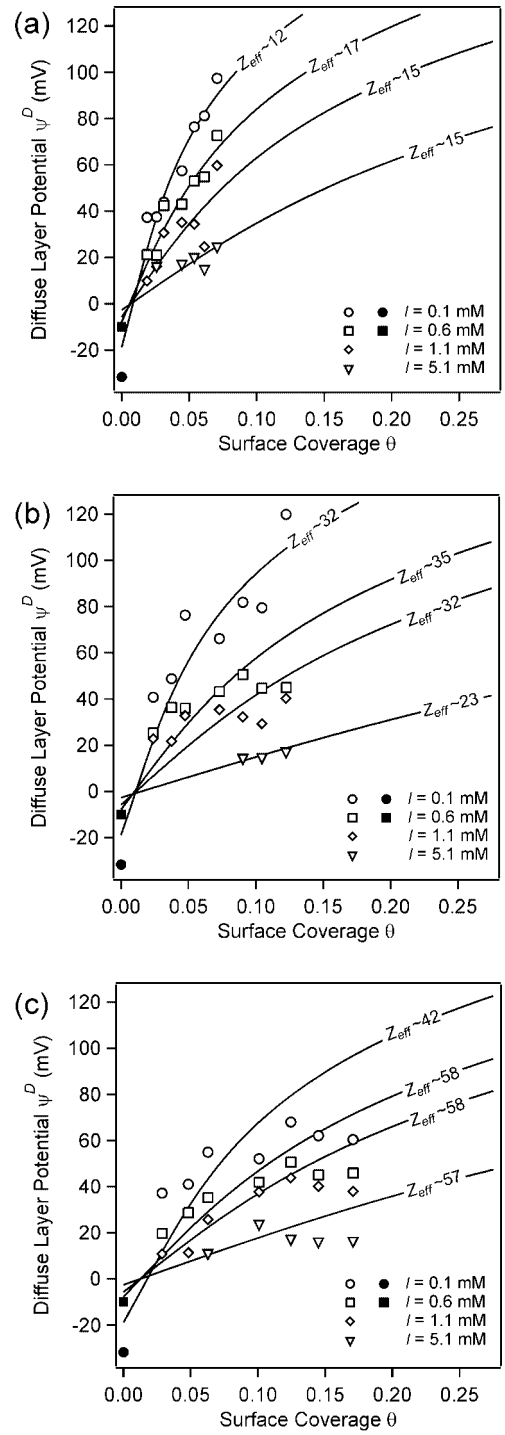

Figure 9. Diffuse layer potentials of silica surfaces coated by PAMAM dendrimers at pH 4 for different ionic strengths as a function of surface coverage. The data for different generations are represented in (a) G6, (b) G8, and (c) G10. The measurements for the dendrimer coated substrates (open symbols) are compared with the bare substrates (solid symbols). The solid lines represent the fits of the diffuse layer with the smeared-out charge model at the respective ionic strength (see eqs 3 and 4).

Figure 9 shows the diffuse layer potentials obtained from the fits of the force profiles as a function of the dendrimer surface coverage for different ionic strengths. The individual graphs show these results for different generations of PAMAM dendrimers (G6, G8, and G10). The measured diffuse layer potentials for the bare silica surface at the lowest ionic strength

are included as well ($\theta = 0$). In spite of some scatter, the data clearly show that the diffuse layer potential increases with increasing surface coverage and decreasing ionic strength. These results reiterate the good reproducibility of the data, and that effects due to the lateral heterogeneities are minor indeed.

The measured potentials are in good agreement with force measurements for adsorbed PAMAM dendrimer layers in the sphere-sphere geometry.[50] This study reports a diffuse layer potential of +98 mV for G6 at coverage of 0.14 and a potential of +70 mV for G10 at coverage of 0.37 measured in a monovalent electrolyte solution of an ionic strength of 0.1 mM and of pH 4.

A similar increase of diffuse layer potentials with decreasing ionic strength was observed by the colloidal probe technique for different preadsorbed polyelectrolyte layers, including poly(ethyleneimine)[31] and poly(vinylamine).[25] One can equally observe that dendrimers of lower generations lead to higher surface potentials. This trend can be related to progressive ion condensation of anions to the dendrimers with their increasing generation, and will be discussed in more detail further below.

On the basis of the present data, one can also roughly estimate the position of charge reversal point. For G10, it occurs near a coverage of $\theta \approx 0.02$. This point appears to shift to lower surface coverage with decreasing dendrimer generation. However, the present approach does not allow studying the interaction forces near this point, and thus these estimates remain tentative.

Effective Dendrimer Charge. From measured diffuse layer potentials, one can estimate the effective charge of the dendrimers on the surface based on a simple smeared-out charge model. For sufficiently large separation distances, one can assume that the surface charge heterogeneities become unimportant, and that the diffuse layer potential originates from an laterally averaged surface charge density.[65] For the present system, the average surface density is the sum of the surface charge density of the silica surface σ_0 and the contribution of the adsorbed dendrimers, namely

$$\sigma = \sigma_0 + \frac{eZ_{\text{eff}}}{\pi a^2}\theta \tag{3}$$

where Z_{eff} is the effective charge of a dendrimer in units of elementary charge e and πa^2 its contact area. From this surface charge density, the diffuse layer potential can be calculated with the inverse Grahame equation[13,14]

$$\psi_d = \frac{2kT}{e}\,\text{asinh}\left(\frac{e\sigma}{2kT\epsilon\epsilon_0\kappa}\right) \tag{4}$$

Within this smeared-out charging model, the effective charge Z_{eff} is the only adjustable parameter, as all other parameters can be determined from independent measurements. The dendrimer diameter in the adsorbed state is known from AFM imaging (see Table 1).[43] The Debye length κ^{-1} can be well estimated from on the ionic strength with eq. (1) as demonstrated in Figure 8. The charge density of the bare silica surface was reported to be $\sigma_0 = -0.4$ mC/m^2 at pH 4 from direct force measurements.[69] This value is close to the prediction of the classical 1-pK basic Stern model with the standard parameters.[70,71]

The fits of the data with this model are shown in Figure 9 as solid lines. The region of the fit was restricted to the regime of low to intermediate surface coverage ($0 < \theta < 0.10$). Given the scatter in the data, the fits provide a relatively good description in this region. The fitted effective charges are indicated in the graphs, and they are quite independent of the different ionic strengths considered. Their values at an ionic strength of 1.1 mM are reported in Table 2. One further notes that the effective charges increase with increasing generation.

Table 2. Charge Characteristics As Obtained by the Different Techniques at an Ionic Strength of 1.1 mM

	bare charge Z from structural formula	effective charge Z_{eff} experimental	theoretical[a]	ratio of experimental to theoretical effective charge
G6	510	15	34	0.44
G8	2046	32	54	0.59
G10	8190	58	84	0.69

[a] Calculated from eq 5.

At high surface coverage, the diffuse layer potentials do not increase as strongly with the coverage as predicted by the smeared-out charging model. This effect is particularly pronounced for high generations, whereby the potential seems to reach a plateau at high coverage. While the smeared-out charging model assumes that the adsorbed dendrimers can be considered as independent entities, these deviations indicate that this assumption become problematic at higher coverage. One might suppose that the overlapping diffuse layers of the adsorbed dendrimers induce additional screening, reducing the effective charge even further. However, the detailed analysis of such effects goes beyond the scope of this study.

Let us first compare the measured effective charges with the number of charged groups on the dendrimers in solution. This quantity is also referred to as the bare charge Z (see Table 2). One should note that the bare charge may decrease substantially in basic conditions due to dissociation of protonated amine groups, but in the present acidic conditions at pH 4, basically all groups are charged.[37] When the effective charge Z_{eff} obtained from AFM measurements is compared with the bare charge Z from the dendrimer structure, one finds that the effective charge is substantially smaller than the bare charge (see Table 2).

The small value of the effective charge can be explained by counterion condensation.[1,72] Dendrimers are highly positively charged, and they accumulate a substantial amount of anions close to their surface. However, the neutralization of the charged groups by these anions is not complete, and a diffuse layer forms around the dendrimer. This diffuse layer can be thought as being induced by a fictitious particle carrying an effective charge. For G10, the effective charge Z_{eff} is less than 1% of the bare charge Z. In other words, more than 99% of the charged groups are neutralized by anions. Furthermore, this fraction decreases with decreasing generation, suggesting that cationic charges within smaller dendrimers are less well neutralized and that they bind a smaller fraction of anions. For this reason, dendrimers of lower generations lead to higher surface potentials than higher generation dendrimers at a given surface coverage. One should note that the surface cannot be the origin of such charge reduction, as the surface will tend to deprotonate the dendrimers even further, leading to their full dissociation in the adsorbed state.[73]

The concept of effective or renormalized charge has been discussed in detail at various levels of approximation for charged rods, planar interfaces, and spherical particles.[1,72,74−79] The simplest way to estimate effective charges is to treat the charge distribution by PB theory and to extract the effective charge from its linearized version, the Debye−Hückel theory. Within this approach one finds that for high charge densities, the effective charge saturates at a limiting value, while for low charge densities it coincides with the bare charge. For a sphere, the saturation value of the effective charge is given by[78,79]

$$Z_{\text{eff}} = (\tilde{a}/L_{\text{B}})(4\kappa\tilde{a} + 6) \tag{5}$$

where $L_{\text{B}} = e^2/(4\pi\varepsilon\varepsilon_0 kT) \approx 0.72$ nm is the Bjerrum length and $\tilde{a}$ is the radius of the particle or the spherical molecule.

The values of the effective charged predicted by PB theory are compared with the experimental values based on direct force

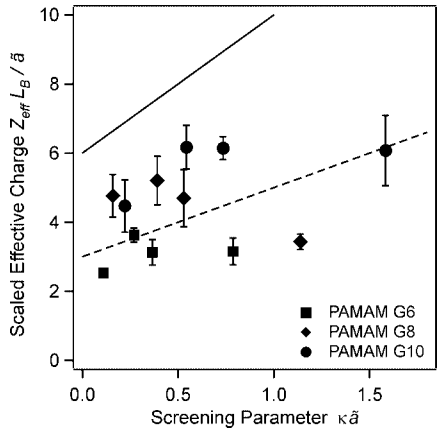

Figure 10. Comparison of the experimental effective charges obtained from force measurements with theoretical values expected for dendrimers in solution. The solid line corresponds to the theoretical values from PB theory (see eq 5), while the dashed line corresponds to half of this value.

measurements in Table 2 at an ionic strength of 1.1 mM. In eq. (5) we have used the dendrimer radius, which was determined in solution by dynamic light scattering (see Table 1). Figure 10 compares the normalized effective charge $Z_{eff}L_B/\tilde{a}$ as a function of the screening parameter $\kappa\tilde{a}$ where all data should collapse on a straight line given by eq. (5). One can see that the experimental and theoretical values lie within the same order of magnitude, but the experimental values are about a factor of 2 lower than the theoretical ones. Moreover, the ionic strength dependence of the theoretical prediction of eq. (5) is stronger than what is observed experimentally. Qualitatively, one can understand this difference by realizing that the PB theory assumes spherical symmetry in bulk, while the diffuse layers of the adsorbed dendrimers interact only through the half-space above the surface. Furthermore, the negatively charged surface neutralizes some of the positive charges within adsorbed dendrimer. These measurements suggest further that the reduction of the effective charge becomes more pronounced with decreasing dendrimer generation, and this effect might be related to the decreasing ratio between the volume of the dendrimer and its contact area. A quantitative treatment of the effective charge of colloidal particles adsorbed on the air−water interface has been put forward recently.[80] However, we are unaware of a similar theory for charged objects close to the water-solid interface to which the present experimental values could be compared.

Conclusions

Forces between negatively charged silica surfaces with adsorbed positively charged dendrimers are measured with the colloidal probe technique. At larger distances, forces between these surfaces are repulsive and consistent with DLVO theory, while attractive non-DLVO forces are observed at shorter distances. The latter forces likely originate from interactions between the oppositely charged patches on the heterogeneously charged surfaces. Due to the compact nature of the dendrimers, attraction due to polymer bridging seems unlikely. Interactions at larger distances can be quantitatively interpreted as originating from electrostatic interactions of overlapping diffuse layers between positively charged surfaces. The variation of diffuse layer potentials with the surface coverage can be rationalized with a smeared-out charge model, whereby the effective charge of the adsorbed dendrimers can be obtained. The effective charges are substantially smaller than the bare charges of the dendrimers, and they are about a factor of 2 lower than effective charges for spherical macromolecules in solution predicted by PB theory.

With estimates of effective charges of adsorbed polyelectrolytes at hand, this framework opens a new way for predicting the magnitude of repulsive double layer forces between adsorbed polyelectrolyte layers quantitatively. While the present approach is only applicable to globular or branched polyelectrolytes of low polydispersity and not too high coverage, an extension might be possible to include higher coverage, polydispersity, and other polyelectrolyte architectures.

Acknowledgment. This research was supported by the Swiss National Science Foundation and the University of Geneva. We acknowledge useful discussions with Piotr Warszynski.

References and Notes

(1) Dautzenberg, H.; Jaeger, W.; Kotz, J.; Philipp, B.; Seidel, C.; Stscherbina, D. *Polyelectrolytes: Formation, Characterization and Application*; Hanser Publishers: New York, 1994.
(2) Leong, Y. K.; Scales, P. J.; Healy, T. W.; Boger, D. V. *Colloids Surf. A* **1995**, *95*, 43–52.
(3) Bolto, B.; Gregory, J. *Water Res.* **2007**, *41*, 2301–2324.
(4) *Retention aids*, 2nd ed.; Horn, D.; Linhart, F., Eds.; Blackie Academic and Professional: London, 1996.
(5) Borkovec, M.; Papastavrou, G. *Curr. Opin. Colloid Interface Sci.* **2008**, *13*, 429–437.
(6) Chen, K. L.; Mylon, S. E.; Elimelech, M. *Environ. Sci. Technol.* **2006**, *40*, 1516–1523.
(7) Gregory, J. *J. Colloid Interface Sci.* **1973**, *42*, 448–456.
(8) Bouyer, F.; Robben, A.; Yu, W. L.; Borkovec, M. *Langmuir* **2001**, *17*, 5225–5231.
(9) Boroudjerdi, H.; Kim, Y. W.; Naji, A.; Netz, R. R.; Schlagberger, X.; Serr, A. *Phys. Rep.* **2005**, *416*, 129–199.
(10) Grosberg, A. Y.; Nguyen, T. T.; Shklovskii, B. I. *Rev. Mod. Phys.* **2002**, *74*, 329–345.
(11) Verwey, E. J. W.; Overbeek, J. T. G. *Theory of Stability of Lyophobic Colloids*; Elsevier: Amsterdam, 1948.
(12) Derjaguin, B.; Landau, L. D. *Acta Phys. Chim.* **1941**, *14*, 633–662.
(13) Russel, W. B.; Saville, D. A.; Schowalter, W. R. *Colloidal Dispersions*; Cambridge University Press: Cambridge, U.K., 1989.
(14) Elimelech, M.; Gregory, J.; Jia, X.; Williams, R. A. *Particle Deposition and Aggregation: Measurement, Modeling, and Simulation*; Butterworth-Heinemann Ltd.: Oxford, U.K., 1995.
(15) Kleimann, J.; Gehin-Delval, C.; Auweter, H.; Borkovec, M. *Langmuir* **2005**, *21*, 3688–3698.
(16) Ashmore, M.; Hearn, J. *Langmuir* **2000**, *16*, 4906–4911.
(17) Walker, H. W.; Grant, S. B. *Colloids Surf. A* **1996**, *119*, 229–239.
(18) Gillies, G.; Lin, W.; Borkovec, M. *J. Phys. Chem. B* **2007**, *111*, 8626–8633.
(19) Bauer, D.; Buchhammer, H.; Fuchs, A.; Jaeger, W.; Killmann, E.; Lunkwitz, K.; Rehmet, R.; Schwarz, S. *Colloids Surf. A* **1999**, *156*, 291–305.
(20) Schwarz, S.; Jaeger, W.; Paulke, B. R.; Bratskaya, S.; Smolka, N.; Bohrisch, J. *J. Phys. Chem. B* **2007**, *111*, 8649–8654.
(21) Poptoshev, E.; Claesson, P. M. *Langmuir* **2002**, *18*, 2590–2594.
(22) Poptoshev, E.; Rutland, M. W.; Claesson, P. M. *Langmuir* **1999**, *15*, 7789–7794.
(23) Dahlgren, M. A. G.; Waltermo, A.; Blomberg, E.; Claesson, P. M.; Sjostrom, L.; Akesson, T.; Jonsson, B. *J. Phys. Chem.* **1993**, *97*, 11769–11775.
(24) Hartley, P. G.; Scales, P. J. *Langmuir* **1998**, *14*, 6948–6955.
(25) Kirwan, L. J.; Maroni, P.; Behrens, S. H.; Papastavrou, G.; Borkovec, M. *J. Phys. Chem. B* **2008**, *112*, 14609–14619.
(26) Dejeu, J.; Buisson, L.; Guth, M. C.; Roidor, C.; Membrey, F.; Charraut, D.; Foissy, A. *Colloids Surf. A* **2006**, *288*, 26–35.
(27) Roiter, Y.; Minko, S. *J. Phys. Chem. B* **2007**, *111*, 8597–8604.
(28) Hugel, T.; Grosholz, M.; Clausen-Schaumann, H.; Pfau, A.; Gaub, H.; Seitz, M. *Macromolecules* **2001**, *34*, 1039–1047.
(29) Friedsam, C.; Seitz, M.; Gaub, H. E. *J. Phys. Condes. Matter* **2004**, *16*, S2369−S2382.
(30) Hugel, T.; Rief, M.; Seitz, M.; Gaub, H. E.; Netz, R. R. *Phys. Rev. Lett.* **2005**, *94*, 048301.
(31) Pericet-Camara, R.; Papastavrou, G.; Behrens, S. H.; Helm, C. A.; Borkovec, M. *J. Colloid Interface Sci.* **2006**, *296*, 496–506.
(32) Pfau, A.; Schrepp, W.; Horn, D. *Langmuir* **1999**, *15*, 3219–3225.
(33) Schneider, M.; Zhu, M.; Papastavrou, G.; Akari, S.; Mohwald, H. *Langmuir* **2002**, *18*, 602–606.
(34) Tomalia, D. A.; Frechet, J. M. J. *J. Polym. Sci. Pol. Chem.* **2002**, *40*, 2719–2728.
(35) Ballauff, M.; Likos, C. N. *Angew. Chem., Int. Ed.* **2004**, *43*, 2998–3020.

(36) Tomalia, D. A.; Baker, H.; Dewald, J.; Hall, M.; Kallos, G.; Martin, S.; Roeck, J.; Ryder, J.; Smith, P. *Macromolecules* **1986**, *19*, 2466–2468.
(37) Cakara, D.; Kleimann, J.; Borkovec, M. *Macromolecules* **2003**, *36*, 4201–4207.
(38) Tully, D. C.; Frechet, J. M. J. *Chem. Commun.* **2001**, 1229–1239.
(39) Betley, T. A.; Banaszak Holl, M. M.; Orr, B. G.; Swanson, D. R.; Tomalia, D. A.; Baker, J. R. *JrLangmuir* **2001**, *17*, 2768–2773.
(40) Rahman, K. M. A.; Durning, C. J.; Turro, N. J.; Tomalia, D. A. *Langmuir* **2000**, *16*, 10154–10160.
(41) Kleijn, J. M.; Barten, D.; Cohen Stuart, M. A. *Langmuir* **2004**, *20*, 9703–9713.
(42) Esumi, K.; Fujimoto, N.; Torigoe, K. *Langmuir* **1999**, *15*, 4613–4616.
(43) Pericet-Camara, R.; Papastavrou, G.; Borkovec, M. *Langmuir* **2004**, *20*, 3264–3270.
(44) Pericet-Camara, R.; Cahill, B. P.; Papastavrou, G.; Borkovec, M. *Chem. Commun.* **2007**, 266–268.
(45) Cahill, B. P.; Papastavrou, G.; Koper, G. J. M.; Borkovec, M. *Langmuir* **2008**, *24*, 465–473.
(46) Lin, W.; Galletto, P.; Borkovec, M. *Langmuir* **2004**, *20*, 7465–7473.
(47) Sakai, K.; Sadayama, S.; Yoshimura, T.; Esumi, K. *J. Colloid Interface Sci.* **2002**, *254*, 406–409.
(48) Hiraiwa, D.; Yoshimura, T.; Esumi, K. *J. Colloid Interface Sci.* **2006**, *298*, 982–986.
(49) Kern, W.; Puotinen, D. A. *RCA Rev.* **1970**, *31*, 187.
(50) Rentsch, S.; Pericet-Camara, R.; Papastavrou, G.; Borkovec, M. *Phys. Chem. Chem. Phys.* **2006**, *8*, 2531–2538.
(51) Barrett, S.; Bickmore, B. R.; Rufe, E.; Hochella, M. F.; Torzo, G.; Cerolini, D. *J. Comput. Assisted Microsc.* **1998**, *10*, 77–82.
(52) Butt, H. J.; Cappella, B.; Kappl, M. *Surf. Sci. Rep.* **2005**, *59*, 1–152.
(53) Hutter, J. L.; Bechhoefer, J. *Rev. Sci. Instrum.* **1993**, *64*, 1868–1873.
(54) Chon, J. W. M.; Mulvaney, P.; Sader, J. E. *J. Appl. Phys.* **2000**, *87*, 3978–3988.
(55) Pericet-Camara, R.; Papastavrou, G.; Behrens, S. H.; Borkovec, M. *J. Phys. Chem. B* **2004**, *108*, 19467–19475.
(56) Betley, T. A.; Hessler, J. A.; Mecke, A.; Banaszak Holl, M. M.; Orr, B. G.; Uppuluri, S.; Tomalia, D. A.; Baker, J. R., Jr. *Langmuir* **2002**, *18*, 3127–3133.
(57) Ducker, W. A.; Senden, T. J.; Pashley, R. M. *Langmuir* **1992**, *8*, 1831–1836.
(58) Adamczyk, Z.; Warszynski, P. *Adv. Colloid Interface Sci.* **1996**, *63*, 41–149.
(59) Adamczyk, Z. *Adv. Colloid Interface Sci.* **2003**, *100*, 267–347.
(60) Semmler, M.; Mann, E. K.; Ricka, J.; Borkovec, M. *Langmuir* **1998**, *14*, 5127–5132.
(61) Ko, C. H.; Bhattacharjee, S.; Elimelech, M. *J. Colloid Interface Sci.* **2000**, *229*, 554–567.
(62) Miyahara, M.; Watanabe, S.; Gotoh, Y.; Higashitani, K. *J. Chem. Phys.* **2004**, *120*, 1524–1534.
(63) Hartley, P. G.; Larson, I.; Scales, P. J. *Langmuir* **1997**, *13*, 2207–2214.
(64) Vigil, G.; Xu, Z. H.; Steinberg, S.; Israelachvili, J. *J. Colloid Interface Sci.* **1994**, *165*, 367–385.
(65) Miklavic, S. J.; Chan, D. Y. C.; White, L. R.; Healy, T. W. *J. Phys. Chem.* **1994**, *98*, 9022–9032.
(66) Kekicheff, P.; Spalla, O. *Phys. Rev. Lett.* **1995**, *75*, 1851–1854.
(67) Hiemstra, T.; de Wit, J. C. M.; van Riemsdijk, W. H. *J. Colloid Interface Sci.* **1989**, *133*, 105–117.
(68) Kobayashi, M.; Juillerat, F.; Galletto, P.; Bowen, P.; Borkovec, M. *Langmuir* **2005**, *21*, 5761–5769.
(69) Radtchenko, I. L.; Papastavrou, G.; Borkovec, M. *Biomacromolecules* **2005**, *6*, 3057–3066.
(70) Hiemstra, T.; van Riemsdijk, W. H.; Bolt, G. H. *J. Colloid Interface Sci.* **1989**, *133*, 91–104.
(71) Kobayashi, M.; Skarba, M.; Galletto, P.; Cakara, D.; Borkovec, M. *J. Colloid Interface Sci.* **2005**, *292*, 139–147.
(72) Oosawa, F. *Polyelectrolytes*; Marcel Dekker, Inc.: New York, 1971.
(73) Cakara, D.; Chassagne, C.; Gehin-Delval, C.; Borkovec, M. *Colloids Surf. A* **2007**, *294*, 174–180.
(74) Lifson, S.; Katchalsky, A. *J. Polymer Sci*. **1954**, *13*, 43−55.
(75) Alexander, S.; Chaikin, P. M.; Grant, P.; Morales, G. J.; Pincus, P.; Hone, D. *J. Chem. Phys.* **1984**, *80*, 5776–5781.
(76) Groot, R. D. *J. Chem. Phys.* **1991**, *95*, 9191–9203.
(77) Gisler, T.; Schulz, S. F.; Borkovec, M.; Sticher, H.; Schurtenberger, P.; D'Aguanno, B.; Klein, R. *J. Chem. Phys.* **1994**, *101*, 9924–9936.
(78) Chew, W. C.; Sen, P. S. *J. Chem. Phys.* **1982**, *77*, 2042–2044.
(79) Aubouy, M.; Trizac, E.; Bocquet, L. *J. Phys. A* **2003**, *36*, 5835–5840.
(80) Frydel, D.; Dietrich, S.; Oettel, M. *Phys. Rev. Lett.* **2007**, *99*, 118302.

MA802374Z